

Unsteady Characteristics of Supersonic Jet Flow Issuing from Annular Nozzle

Nianru YANG*, Tadatomo KOJIMA**

A study was performed by experiment and numerical analysis on an unsteady character of a supersonic jet flow issuing from an annular nozzle. It was clarified by the experiment that the difference from the shape of the nozzles in the center part of the annular influenced the flow field and the pressure vibration. Furthermore, the vortex formed in low-pressure region of the flow in the nozzle exit was clarified by the numerical analysis. Especially, it was clarified that the shape of the nozzles influenced the vortex and the pressure vibration.

Keywords : Shock wave, Numerical analysis, Exhaust silencer, Compressible flow, Separation, Supersonic flow, Unsteady flow, Annular nozzle

1. Introduction

Studies were provided well on various fields about a supersonic jet flow issuing from an annular nozzle or a single nozzle. The nozzles were used as industrial nozzles on various fields, but the detail character is still not clear.

This study was clarified by experiment and numerical analysis about an unsteady character of a supersonic jet flow issuing from an annular nozzle. Especially, it was clarified by the experiment that the difference from the shape of the nozzles in the center part of an annular influenced the flow field and the pressure vibration.

In addition, it was clarified by the numerical analysis that the situation of the flow was in the exit of the nozzles and the vortex field was formed in the low-pressure region. Especially, it was done by the numerical analysis that the shape of the nozzles which was in the point of the center part and the difference of the pressure of the stagnation tank influenced the velocity vector, and it was clarified on the vortex formation and the pressure vibration.

2. Experiment method and Analysis method

Two nozzles were used to make an experiment and a numerical analysis in this study. One was a circle type on the point. The other was a flat type on the point.

For measuring total pressure vibration, a micro semiconductor pressure transducer was installed on the point of the total pressure probe. And the frequency analysis of the total pressure vibration was taken by FFT analyzer.

In the experiment, the central axis of nozzles was made as X axis and the vertical cross section was made as Z axis. The total pressure vibration was measured for jetting direction from $X/d = 0$ to 7 and for vertical direction from $Z/d = 0$ to 0.5.

It was analyzed with momentum equation, equation of energy and Finite Volume Method (FVM).

In the experiment and the numerical analysis, it was made with pressure ratio $Po/Pa = 3.0, 6.0, 10.0,$ and 20.0 . The pressure ratio Po/Pa was that stagnation pressure Po was divided by atmospheric pressure Pa .

*近畿大学大学院システム工学研究科

**近畿大学工学部知能機械工学科

Graduate School of Systems Engineering, Kinki University
Department of Intelligent Mechanical Engineering,
School of Engineering, Kinki University

3. Experiment results and Consideration

3.1 Total pressure vibration as $Po/Pa = 3.0$

The total pressure vibration of the nozzle 1 as the pressure ratio $Po/Pa = 3.0$ is shown in Figure 1 and Figure 2.

As from $X/d = 0.1$ to 1.2 and $Po/Pa = 3.0$ show in Figure 1, remarkable total pressure vibration was seen near from $X/d = 0.5$ to 1.2 within the central axis and $Z/d = 0.2$. It is thought that the annular jets were invited each other by the pressure decrease of the close space near the exit of the annular nozzle, and the collision and the confluence caused the vibration of the flow. Remarkable total pressure vibration was seen near the jet boundary layer from $X/d = 0.5$ to 1.2 within from $Z/d = 0.3$ to 0.4 . The reason is that the disorder of the vicinity of the jet boundary layer was involved by surrounding flows. Moreover, in the region from $X/d = 0.5$ to 1.2 within $Z/d = 0.5$, the remarkable total pressure vibration was not seen. It was the measuring position in the outside of the jet boundary layer.

As from $X/d = 1.5$ to 6.0 and $Po/Pa = 3.0$ shown in Figure 2, remarkable total pressure vibration was seen near from $X/d = 1.5$ to 2.0 within the central axis and $Z/d =$ from 0.0 to 0.4 . It is thought that the flows were vibrated by the disorder of the confluence of the annular nozzle. Moreover, after $X/d = 3.0$, there is a tendency that the total pressure vibration gradually becomes small of velocity decrease.

3.2 Total pressure vibration as $Po/Pa = 6.0$

The pressure vibration of the nozzle 1 as the pressure ratio $Po/Pa = 6.0$ is shown in Figure 3 and Figure 4.

As from $X/d = 0.1$ to 1.2 and $Po/Pa = 6.0$ shown in Figure 3, remarkable total pressure vibration was seen near from $X/d = 0.5$ to 1.2 within the central axis and $Z/d =$ from 0.2 to 0.3 . The total pressure vibration is remarkable than $Po/Pa = 3.0$. Moreover, remarkable total pressure vibration was seen immediately after the exit of the annular nozzle near from $X/d = 0.1$ to 0.3 within $Z/d =$ from 0.4 to 0.5 and $X/d = 0.5$ to 1.2 within $Z/d = 0.4$. Comparing with $Po/Pa = 3.0$, it is known that the total pressure vibration is bigger and the position of the flow disorder is changed by the rolling of surrounding flows.

As from $X/d = 1.5$ to 7.0 and $Po/Pa = 6.0$ shown in the Figure 4, remarkable total pressure vibration was seen near from $X/d = 1.5$ except the outside of the boundary layer $Z/d = 0.5$. To be shown in figure 3, remarkable total pressure vibration was seen near the

exit of the annular nozzle from $X/d = 0.1$ to 1.2 . But total pressure vibration is small after $X/d = 1.5$ and a big difference is not seen in the measured region.

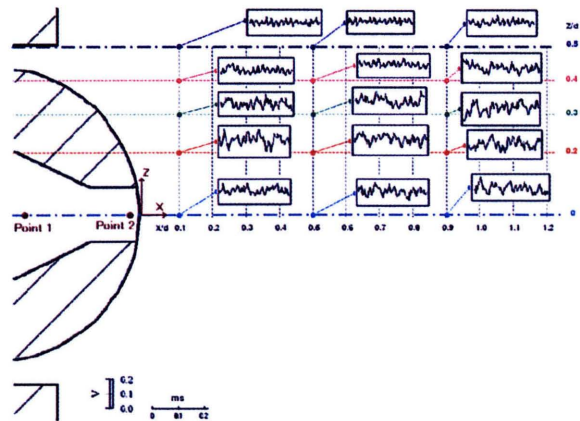


Fig.1 Total pressure vibration for nozzle 1 ($Po/Pa = 3.0, X/d = 0.1 \sim 1.2$)

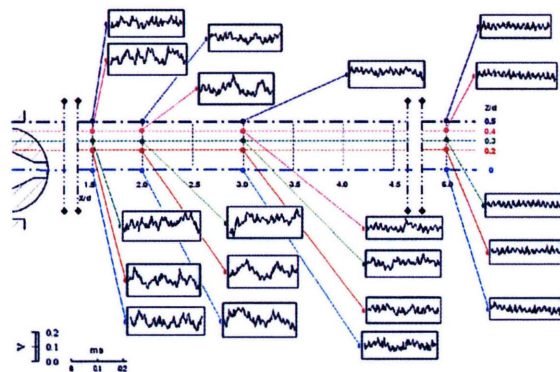


Fig.2 Total pressure vibration for nozzle 1 ($Po/Pa = 3.0, X/d = 1.5 \sim 6.0$)

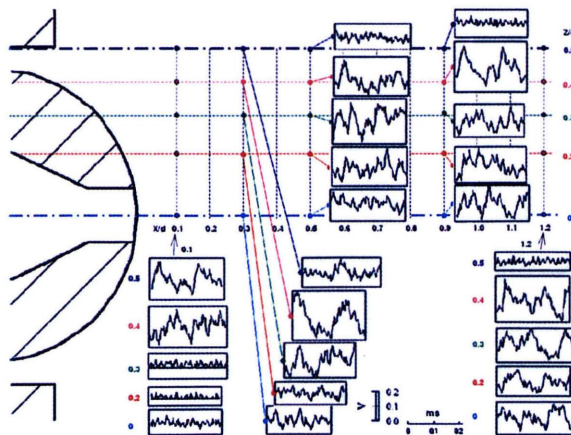


Fig.3 Total pressure vibration for nozzle 1 ($Po/Pa = 6.0, X/d = 0.1 \sim 1.2$)

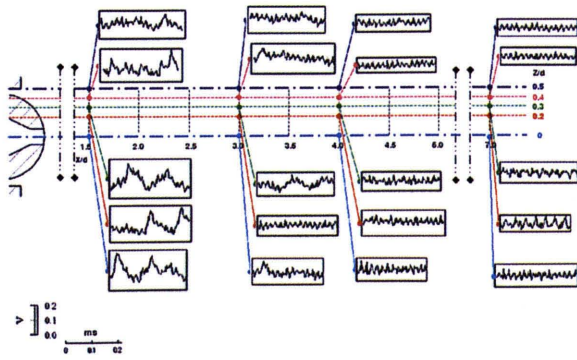


Fig.4 Total pressure vibration for nozzle 1
($Po/Pa = 6.0, X/d = 1.5\sim 6.0$)

3.3 Time-averaged total pressure distribution as $Po/Pa = 3.0$

The time-averaged total pressure distribution of the jet cross section of the nozzle 1 as the pressure ratio $Po/Pa = 3.0$ is shown in Figure 5.

The annular jet became concave distribution in the region that the jet was issuing immediately after the exit of the nozzle from $X/d = 0.1$ to 1.0 . The total pressure was the biggest at the $Z/d = \pm 0.2$. The total pressure decreased in the low-pressure vortex region which was formed near the point of the contrail nozzle, and it decreased most at the $Z/d = 0.0$. Especially, the pressure decrease was mostly remarkable at the $X/d = 0.5$ and 0.7 within $Z/d = 0.0$. Moreover, the annular jet became a single jet by inviting them each other from $Z/d = 2.0$ to 3.0 .

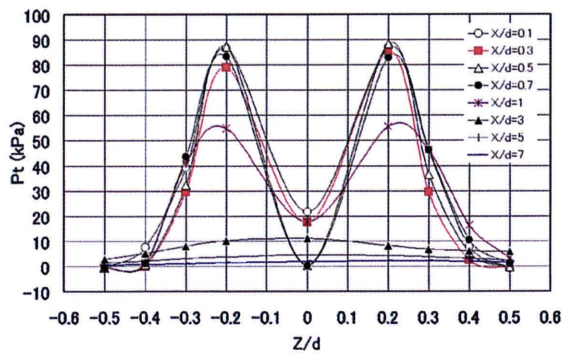


Fig.5 Total pressure distribution for nozzle 1
($Po/Pa = 3.0$)

4. CFD results and Consideration

4.1 The annular jet flow issuing from nozzle 1

The outside shape of the annular nozzle was designed by paralleling X axis.

The velocity vector of the nozzle 1 near the nozzle exit is shown from Figure 6 to Figure 9.

As $Po/Pa = 3.0$ shown in Figure 6, the annular jet issuing from nozzle 1 became an attached jet along the nozzle, and separated at a point to form a pair of vortices. The separation point, the low-pressure vortex region, and the disorder of the flow filed near the boundary layer were observed by the result of the numerical analysis. It corresponds almost with the amplitude of the total pressure vibration shown in Figure 1.

As $Po/Pa = 6.0$ shown in Figure 7, the swelling of the annular was increased a little than $Po/Pa = 3.0$. The separation point, the low-pressure vortex region, and the disorder of the flow filed near the boundary layer were observed by the result of the numerical analysis. It corresponds almost with the amplitude of the total pressure vibration shown in Figure 3.

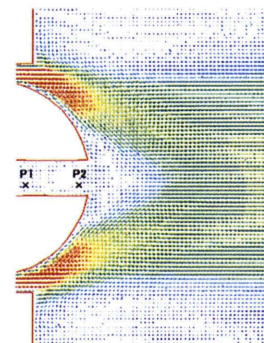


Fig.6 Velocity vector for nozzle 1($Po/Pa = 3.0$)

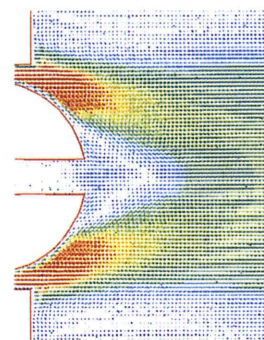


Fig.7 Velocity vector for nozzle 1($Po/Pa = 6.0$)

As $Po/Pa = 10.0$ shown in Figure 8, the swelling of the annular was still increased, and the separation point shifted backward.

As $Po/Pa = 20.0$ shown in Figure 9, the jet expanded rapidly and its separation point still shifted backward.

According to the above-mentioned results, there is a tendency that the separation point shifts backward

and the vortex region becomes small with pressure ratio increasing.

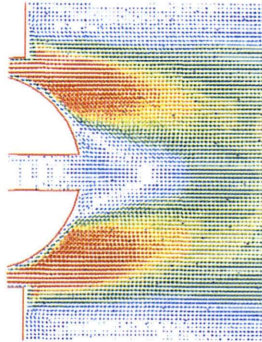


Fig.8 Velocity vector for nozzle 1($P_o/P_a = 10.0$)

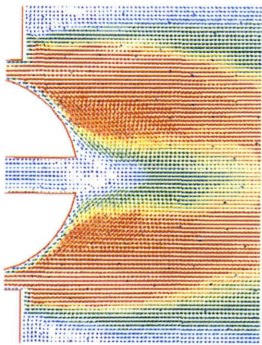


Fig.9 Velocity vector for nozzle 1($P_o/P_a = 20.0$)

4.2 The annular jet flow issuing from nozzle 2

The outside shape of the nozzle is designed to have divergence for easy to accelerate at the exit in high pressure. Only one side is made to Laval shape.

The velocity vector of the nozzle 2 near the nozzle exit is shown from Figure 10 to Figure 13.

As $P_o/P_a = 3.0$ shown in Figure 10, a pair of remarkable vortexes were formed at the point of the nozzle.

As $P_o/P_a = 6.0$ shown in Figure 11, the swelling of the annular was increased outside a little than $P_o/P_a = 3.0$.

As $P_o/P_a = 10.0$ shown in Figure 12, the swelling of the annular was still increased than $P_o/P_a = 6.0$. The vortex region became narrow because the jet was rolling toward the flat part, this is, the inside of the edge of the point of the nozzle.

As $P_o/P_a = 20.0$ shown in Figure 13, the vortex region still became narrow because the jet expanded rapidly.

4.3 Pressure about the point of the nozzle

It is shown in Figure 14 that the CFD results of nozzle 1 and nozzle 2 is pointed at the P1 and P2

about the static pressure.

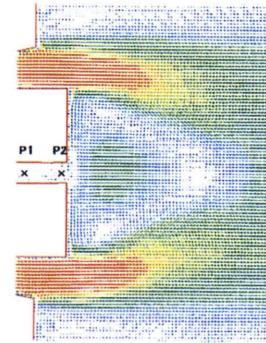


Fig.10 Velocity vector for nozzle 2($P_o/P_a = 3.0$)

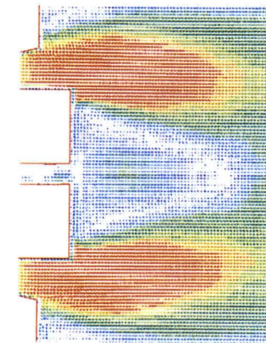


Fig.11 Velocity vector for nozzle 2($P_o/P_a = 6.0$)

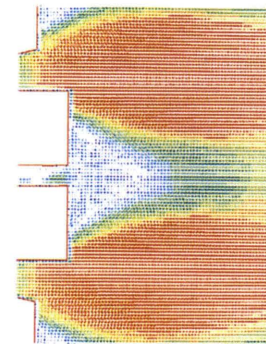


Fig.12 Velocity vector for nozzle 2($P_o/P_a = 10.0$)

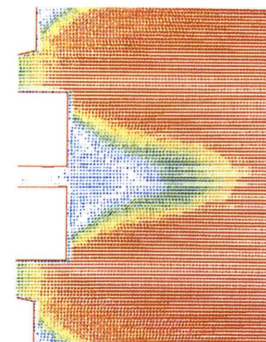


Fig.13 Velocity vector for nozzle 2($P_o/P_a = 20.0$)

In the nozzle 1, the negative pressure is decreasing with increasing stagnation pressure when over $Po/Pa = 10.0$.

In the nozzle 2, because the vortex region is formed at the exit part of the nozzle, there is a tendency that the negative pressure is decreasing with increasing stagnation pressure.

There is a tendency that the negative pressure of the nozzle 2 appears lower than the nozzle 1 by the influence of the vortex region.

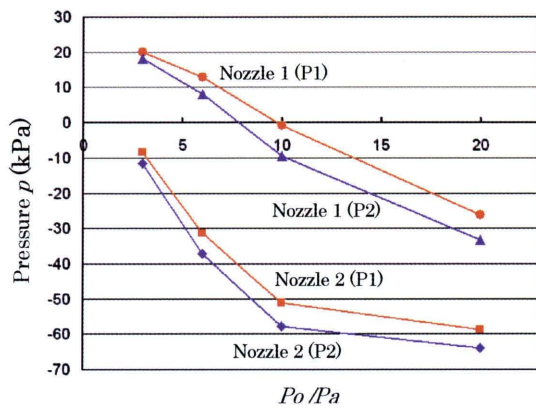


Fig.14 Pressure distribution of P1 and P2

5. Conclusion

- (1) In the annular nozzle where point has roundness, the total pressure vibration is remarkably influenced by separation, collision, confluence, and rolling of surrounding flows.

- (2) With increasing stagnation pressure, the separation point moves and the vortex region becomes narrow
- (3) At the point of flat nozzle, strong vortex region is formed and the vortex region becomes narrow with increasing stagnation pressure.
- (4) In the pressure of the point of nozzles, there is a decreasing tendency with increasing stagnation pressure. On the negative pressure, the nozzle where the point has flat shape is more remarkable than the nozzle where the point has roundness shape.

References

- (1) Akihiko Mitsuishi, Koji Fukagata, Nobuhide Kasagi, Vortex-ring Motion and Mixing Process in a Controlled Confined Coaxial Jet, Lecture thesis collection of Japan Society of Fluid Mechanics, pp. 304-305 (2004)
- (2) Yu Liu, Tadatomo Kojima, Yashshi Fujita, Study on Structure of Pseudo-Shock Waves in Under-Expanded Jet, Journal of the Visualization Society of Japan, Vol.23, Suppl. No.1, pp.53-56 (2003)